Astron. Astrophys. 312, 941–949 (1996)

ASTRONOMY AND ASTROPHYSICS

MWC 314: a high-luminosity peculiar Be star*

Anatoly S. Miroshnichenko

Central Astronomical (Pulkovo) Observatory of the Russian Academy of Sciences, 196140 Saint-Petersburg, Russia (anat@pulkovo.spb.su)

Received 22 May 1995 / Accepted 29 February 1996

Abstract. New broad-band multicolor photometry and optical spectroscopy of the emission-line star MWC 314 = BD +14°3887 as well as a study of its ultraviolet spectrum are reported. It is shown that the star exhibits photometric variability with a quasi-regular component. Main parameters of the star and its envelope are determined from both the spectral energy distribution and emission line analysis. It is concluded that MWC 314 is a highly reddened ($A_V = 5\overset{m}{.}7$) supergiant with strong slow stellar wind. The stellar parameters are: $\log L/L_\odot = 6.2, T_* = 30\,000$ K, $R_* = 50 R_\odot$, which yield an initial mass of about 80 $M_\odot$. The stellar wind has a quite low terminal velocity ($v_\infty = 500$ km s^{-1}, a high mass loss rate ($\dot{M} = 3\,10^{-5} M_\odot$ yr^{-1}), and a structure similar to that of P Cyg. There is no evidence for a dust shell in the vicinity of the object. A comparison of the object's parameters with those of LBVs and B[e]–supergiants is also presented. MWC 314 can be considered as a candidate LBV.

Key words: stars: individual MWC 314 ; mass loss; Be; supergiants; fundamental parameters – ultraviolet: stars

1. Introduction

An increasing number of observations in different spectral ranges has recently allowed to study more deeply objects with circumstellar shells and to discover new groups of them. However, in many cases, the brightest objects or the objects having prominent features turn out to be the most investigated now. At the same time many stars are known to have emission lines and IR excesses which have been studied a little. The object in question – MWC 314 = BD +14°3887 – belongs to the latter ones. Merrill (1927) was the first to pay attention to this star because of the presence of hydrogen and Fe II emissions in its spectrum. Swensson (1942) obtained seven spectrograms of the object (3370-6600 Å, 40-100 Å mm^{-1} near 3933 Å). He has detected interstellar H and K Ca II lines and 4430 Å band, Balmer emissions from Hα to H$_8$, emissions of Na I at 5890 and 5896 Å. Photospheric lines and spectral features of late-type stars were not observed in these spectra. Swensson has estimated a spectral type of the underlying star as gG2-3 or dG4-5 from the spectral energy distribution (SED) in the continuum, and B2 from the degree of excitation. Analysing the results of the IR photometry (HKL-bands), Allen (1973) noted that the SED of MWC 314 corresponds to that of a late-type star but the object may be a symbiotic system or a reddened normal star. Nobody else has determined a more exact spectral classification of this star. Only three optical photometric measurements of this star in the Johnson system have been published (Hiltner 1956; Lee 1970; Haupt & Schroll 1974). Their results are very close (see Table 1). The IRAS fluxes detected only at 12 and 25 μm together with other photometric data allow to construct the SED of MWC 314 in a quite wide spectral range (Fig. 1). It is very similar to that of P Cyg but implies essentially larger reddening. The SED of MWC 314 is also close to that of XX Oph, a binary system containing a hot (B0) and a cool (M-type) star (Lockwood et al. 1975). The object is unknown as a radio source in both continuum and spectral lines. Hence, analysing the information previously obtained for MWC 314 we can conclude that this system must contain, at least, a hot star surrounded by a dense gaseous envelope. To make more definite conclusions we carried out a new extended study of this star.

2. Observations

2.1. Photometry

The photometric $UBVRIJHK$ observations were carried out at the 1 meter (Assy Observatory, 2700 m altitude) and the 60-cm (Almaty, 1400 m altitude, July 1994 only) telescopes of the Fessenkov Astrophysical Institute of the National Academy of Sciences of the Kazakhstan Republic with a two–channel photometer–polarimeter (Bergner et al. 1988) in 1990–1994 (diaphragm 26″). BS 7300 was used as a comparison star. We have obtained 7 $UBVRIJHK$ and 42 $UBVRI$ measurements. The original photometric data were published separately (Bergner et al. 1995). Our observations show that the object is variable in all photometric bands with a mean amplitude of $0\overset{m}{.}3$

* partly based on observations by the International Ultraviolet Explorer collected at the Villafranca Satellite Tracking Station of the European Space Agency

Table 1. Photometric observations of MWC 314

Date	V	$U-B$	$B-V$	$V-R$	$V-I$	Reference
1954	9.90	0.37	1.59	-	-	Hiltner (1956)
1969	9.90	0.33	1.54	1.56	2.76	Lee (1970)
1969	9.85	0.38	1.63	-	-	Haupt & Schroll (1974)
1992[a]	9.92	0.30	1.62	1.46	2.66	Bergner et al. (1995)
1995	9.84	0.23	1.57	1.56	-	Mel'nikov (1995)

[a] mean values from our observations

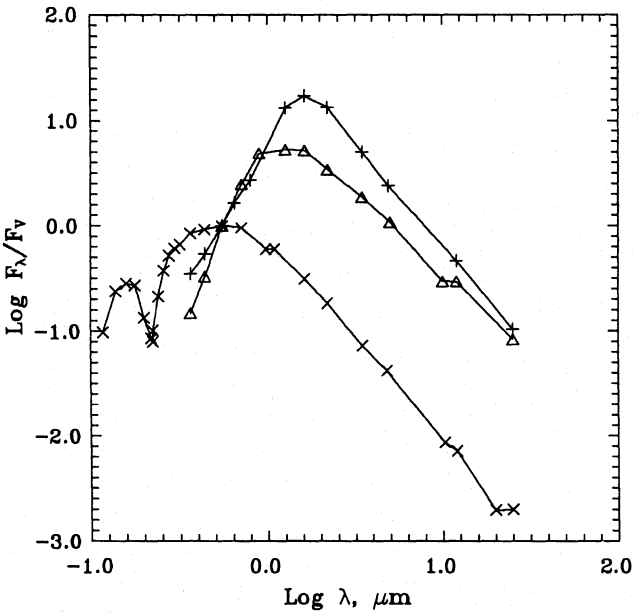

Fig. 1. Spectral energy distribution of MWC 314 (△), P Cyg (×), and XX Oph (+)

(Fig. 2). It was by $\sim 0\overset{m}{.}2$ fainter in the V–band in 1992–1993. At the same time $B-V$ became by $0\overset{m}{.}2$ smaller and $V-R$ by $0\overset{m}{.}1$ larger than during other periods. Our photometry was not frequent enough to conclude on a timescale of such events. The mean brightness level of MWC 314 is very close to that of published observations and proves relative stability of the object on the timescale of years (Table 1). Location of the object in the color-color diagram (Fig. 9) unambiguously shows that it is a highly reddened hot star. Reporting the preliminary results of this study (Miroshnichenko 1994) we pointed out that the Fourier analysis of the light curves in the optical bands performed by means of Deeming's (1975) technique showed the presence of periodical variations with a period of $4\overset{d}{.}16$. The phase curve in the B–band convolved with this period is presented in Fig. 3 where one can see the regular part of the variability. The data sets obtained in short time periods (marked in Fig. 3 by different symbols) demonstrate that the star shows different brightness levels in different periods. However, at the phases close to 0.5 it is usually fainter. In the V–band the picture is similar. In other bands (U, R, I) non-regular variability dominates.

Table 2. Spectroscopic observations of MWC 314

Date	Name	Spectral range	Exp.time
12/Oct./86	A20907	6453 - 7475	1832 s
12/Oct./86	A20908	3984 - 4970	2298 s
14/Oct./86	A21103	6447 - 7472	1523 s
21/Jul./91	A65507	5976 - 7012	1330 s
21/Jul./91	A65508	5976 - 7010	1471 s
21/Jul./91	A65509	4206 - 5234	1582 s
26/Aug./84	lwp4085	1902 - 3199	32 min
31/Oct./84	swp24355	1191 - 1950	180 min
31/Oct./84	lwp4682	1902 - 3199	40 min
02/Jul./92	swp45053	1191 - 1950	480 min
02/Jul./92	lwp23417	1900 - 3298	75 min
02/Jul./92	lwp23418	1900 - 3298	45 min

2.2. Optical spectroscopy

The spectroscopic observations were obtained in October 1986 and in July 1991 at the 6-meter telescope of the Special Astrophysical Observatory of the Russian Academy of Sciences at the Northern Caucasus with the photoelectric scanner (Balega et al. 1979) in the range of 4000-7500 Å with a dispersion of 50Å mm^{-1} (2Å resolution). The log of the observations in both the visual and UV regions (see Sect. 2.3) is presented in Table 2. Our spectra of MWC 314 are very similar to those of Swensson. Their most prominent features are emission lines of H I, He I, Fe II, and interstellar absorptions at λ 4430 Å and λ 6284 Å. The profiles of the hydrogen emissions (Fig. 4) have no absorption components. The Balmer decrement is $I_{H_\alpha} : I_{H_\beta} : I_{H_\gamma} = 1 : 0.060 : 0.0011$. The strong interstellar absorptions confirm a high reddening of the star following from the photometry. These features are easily seen in each spectrum. To find more weak lines we investigated small spectral intervals of nearly 100-200 Å in width where strong lines were excluded and the continuum level was drawn by the least square method. The features with intensities exceeding the noise level (usually about 0.1 of the continuum intensity) and having widths larger than our resolution were suspected as spectral lines. The UV spectral lines were found by the same procedure. The list of identified lines is presented in Tables 3 and 4 for the optical and UV range respectively. Doubtful identifications and uncertain values of line characteristics are marked by colons. The majority of spectral lines detected in the optical wavelength region

Table 3. Identified lines in the optical spectrum of MWC 314

λ_{obs}	Identification	λ_{lab}	W_λ^{1986}, Å	$FWHM^{1986}$, Å	W_λ^{1991}, Å	$FWHM^{1991}$, Å	Type
4103.5	Hδ	4101.737	1.3	4.1			em
4116.6	Si IV 1	4116.104	0.2	1.9			abs
4175.7	Fe II 27	4173.450	0.8	2.7			em
4181.1	Fe II 28,21	4178.855,4183.200	0.9	4.5			em
4208.5	Fe II 22:	4205.480	0.9[a]				em
4225.4	Ca I 2 IS:	4226.728	0.3	1.9	0.8	2.3	abs
4235.5	Fe II 27	4233.167	0.5	3.0			em
4244.4	[Fe II] 21	4244.530			0.6	2.1	em
em							
4283.3	O II 67,Fe I 19:	4283.750,4283.870	1.0	6.7			abs
4295.8	Fe II 28	4296.567			0.8	3.1	em
4323.1	O II 61:	4319.930			1.1	3.1	abs
4340.2	Hγ	4340.458	3.2	4.6	3.8	3.6	em
4386.5	Fe II 26	4386.570			0.7	2.1	em
4430	IS		2.0	9.6	2.9	12.0	abs
4471.3	He I 14	4471.477	0.7	4.3	0.8:	2.8	em
4490.6	Fe II 37	4489.185	1.0	3.8			em
4521.7	Fe II 37	4520.225	0.7	4.1			em
4861.3	Hβ	4861.332			20.0[b]	6.1	em
4922.4	He I 48 + Fe II 42	4921.929,4923.921			2.2	8.9	em
5017.6	He I 4 + Fe II 42	5015.675,5018.434			3.8	5.8	em
6244.7	Fe II 74	6239.950,6247.562			3.4[c]		em
6284	IS				2.7	8.3	abs
6348.2	Si II 2	6347.000			0.4	3.1	em
6370.5	Si II 2	6371.359			0.7	2.6	em
6418.1	Fe II 74	6416.905			0.9	4.4	em
6433.4	Fe II 40	6432.654			1.2	3.6	em
6456.7	Fe II 74	6456.376			1.2	4.6	em
6517.1	Fe II 40	6516.053	2.5	6.7	1.4	4.1	em
6563.8	Hα	6562.817			143.7	5.2	em
6614.1	IS		0.2	1.9	1.0[d]		abs
6680.4	He I 46	6678.149	1.6	4.8	3.3	4.9	em
7065.3	He I 10	7065.188,7065.719	4.4	4.8			em

[a] blend of λ 4208.1 and λ 4210.0 Å
[b] blend with λ 4871.6 Å
[c] blend of λ 6239.5 and λ 6250.1 Å
[d] blend with λ 6609.2 Å

are in emission. The absorption features are mainly interstellar or circumstellar (Ca I 4225 Å, 4283 Å), but some of them (4116 Å and 4323 Å) are probably photospheric. Both these identifications are uncertain since the feature at 4323 Å is situated quite far from the laboratory wavelength of the O II 4320 Å line, and the depth of the feature at 4116 Å is very close to the noise level (Fig. 5). The He I lines (4471, 6678, 7065 Å) are in emission (see for example Fig. 4) and can be used to estimate the object's spectral type. A comparison with the spectra of similar objects (B[e]–supergiants, LBVs) shows that it must be earlier than B2 because only such hot stars have He I lines in emission. Below we show that MWC 314 is a high-luminosity star. The mean expansion velocity derived from the FWHM of unblended lines is about 200 km s^{-1}. Fe II lines are numerous but not strong, while [Fe II] emissions are practically invisible in our spectra. We have only detected weak [Fe II] emission at 4244 Å. A similar situation is observed in the spectra of peculiar high-luminosity stars CD −42°11721 (Hutsemékers & van Drom 1990) and CPD −52°9243 (Winkler & Wolf 1989). This can be explained by a high density of the circumstellar envelope. We had a limited possibility to compare the spectra of 1986 and 1991 because they were obtained in different ranges, with different exposures, and with different integration rates. Thus, for instance, the Balmer emission lines were overexposed in 1986. However, we can see that the lines detected in both observing runs turned out to be stronger in 1991. Such variations are not unusual for the unstable winds of early-type supergiants. Some lines detected in 1991 were not separated from the noise in the 1986 spectra. In any case, we can suppose that the photometric variability of MWC 314 is partly due to the variations of the stellar wind.

Table 4. Identified lines in the UV spectrum of MWC 314

λ_{obs}	Identification	λ_{lab}	W_λ, Å	FWHM,Å	Type
2627.9	Fe II 1	2625.664, 2628.291	5.4	6.0[a]	em
2656.1	Cr II 8	2653.57, 2661.73	4.8	6.2[b]	em
2717.3	Fe II 62	2716.683	1.2	4.2	em
2739.1	Fe II 63	2739.545	1.8	6.3	em
2758.1	Cr II 6	2757.72	1.8	5.4	em
2796.5	Mg II 1	2795.523, 2802.698	6.8	16.2[c]	abs
2824.9	Fe II 3.15	2823.327	1.2	5.5	em
2882.9	Fe II 230	2883.709	0.2	3.0	abs
2893.6	Fe II 230	2894.776	0.3	3.1	em
2907.0	Fe II 60	2907.853	0.2	1.8	abs
2984.8	Fe II 78	2984.831	0.4	3.6	em

[a] blend of λ 2625.0 and λ 2628.8 Å
[b] blend of λ 2654.9 and λ 2662.4 Å
[c] blend of λ 2793.2, λ 2800.7, and λ 2806.2 Å

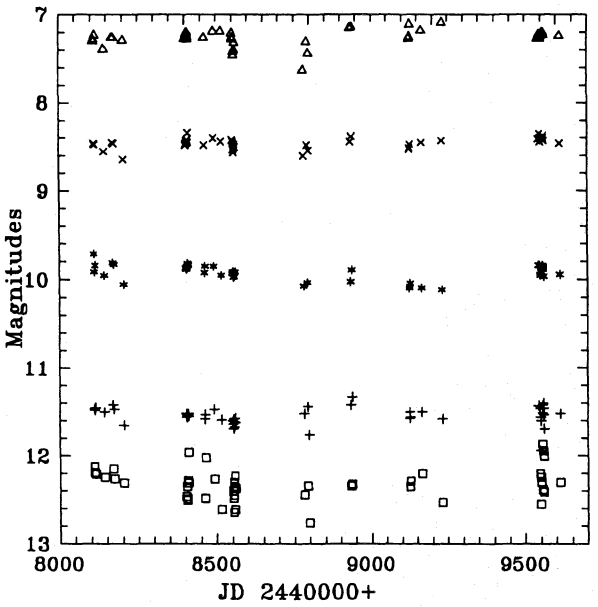

Fig. 2. Light curves of MWC 314 in the optical wavelength bands. From top bottom: I, R, V, B, U. The U-magnitudes are shifted in $0\overset{m}{.}5$ because they are very close to the B-values.

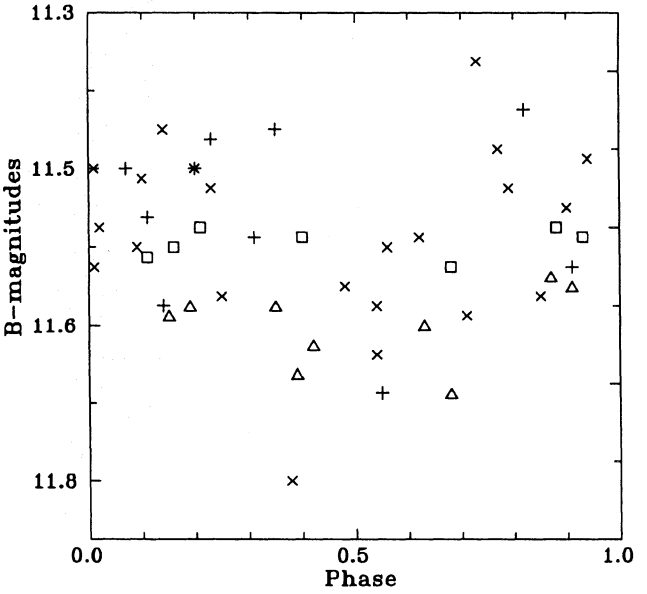

Fig. 3. Phase curve of MWC 314 in the B-band for the $4\overset{d}{.}16$ period. Different symbols represent different periods of observations: JD2448402-2448410 (□), JD2448552-2448561 (△), JD2449542-2449560 (+), other dates (×)

2.3. UV spectroscopy

Low-dispersion spectra of MWC 314 were obtained with different IUE programs in 1984 and 1992 with the LWP and the SWP camera. The short-wavelength part of the spectrum is underexposed and/or contaminated with a strong noise ($\lambda\lambda$ 1200-1700 and $\lambda\lambda$ 1900-2500 Å). Several weak emission lines are visible in the rest of the SWP 24355 spectrum. The LWP spectra resemble each other and show absorption and emission lines of low-ionized species (Table 3). We identified them using the list of UV lines given by Bauer & Stencel (1989). The UV spectrum of MWC 314 (see Fig. 6) is dominated by Fe II lines and is qualitatively similar in the studied range to those of WRA 751, AG and HR Car (de Winter et al. 1992). Only the feature at λ 3025.6 Å observed in all spectra of MWC 314 is not observed in the spectra of the above mentioned stars. We studied UV spectra of some other peculiar Be-supergiants and found a feature at this wavelength which is in absorption in the spectrum of HD 87643 and in emission in the spectrum of HDE 327083. It is difficult to estimate the expansion velocity from the UV data because of poor spectral resolution which is comparable with the FWHM of the lines. The observed fluxes between 2500 and 3200 Å were almost the same in 1984 than in 1992. We used most well recorded parts of the LWP 23417 and SWP 24355 together with the optical photometric data to estimate effective

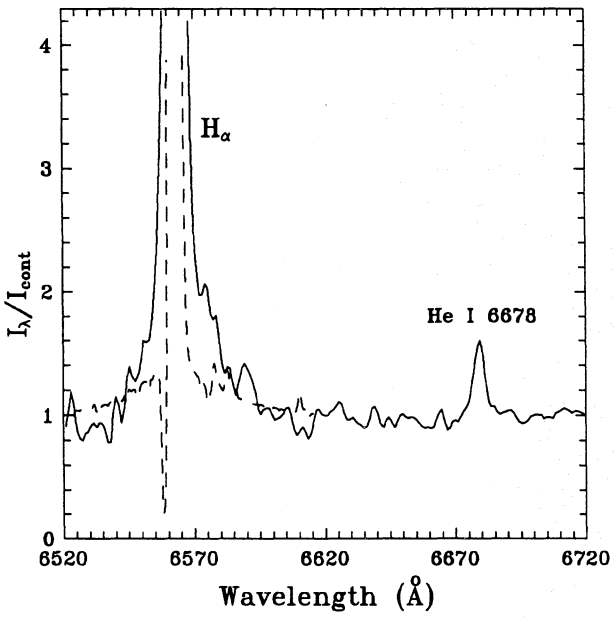

Fig. 4. Hydrogen and helium emissions in the spectrum of MWC 314 . Hα-line of P Cyg is shown by dashed line for comparison.

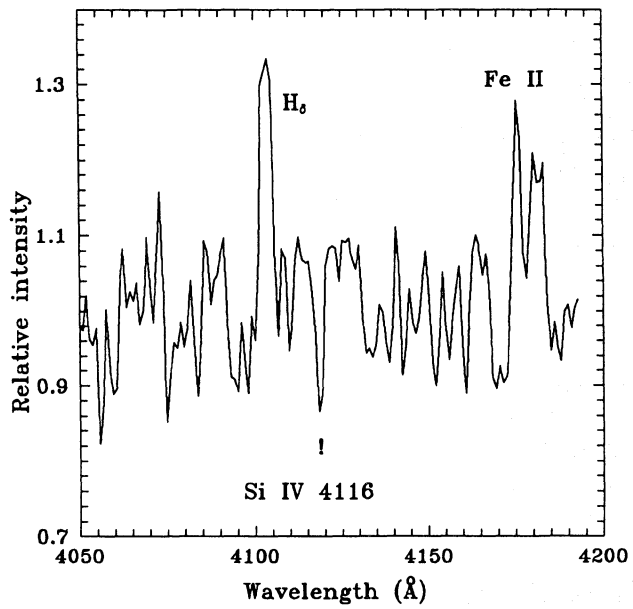

Fig. 5. Weak lines in the spectrum of MWC 314

temperature (T_*) and reddening (A_V) of MWC 314 . Comparison with the Kurucz (1979) models reddened with the Savage & Mathis (1979) interstellar extinction law shows that it is difficult to choose the best model (Fig. 7) because of the noisy spectrum. However, we consider that the lowest temperature model disagrees with the data stronger than other ones. Thus, from the above study of the UV and optical spectra of MWC 314 we can conclude that the object's spectral characteristics are similar to those of other peculiar early-B supergiants having slow dense stellar winds.

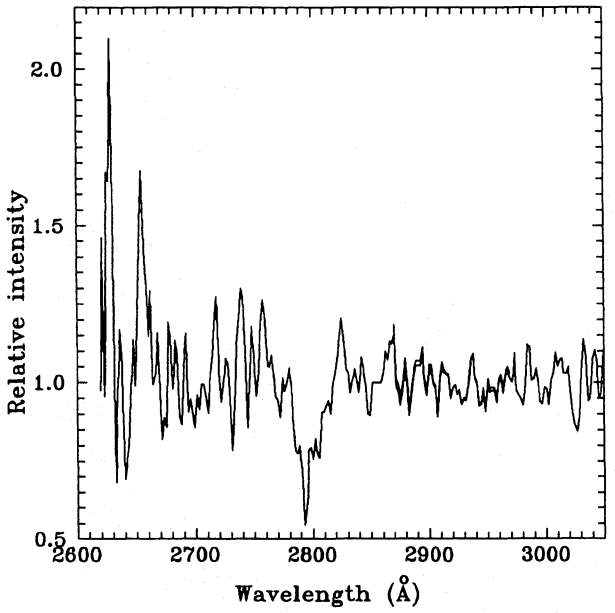

Fig. 6. The normalized low-dispersion IUE spectrum of MWC 314 in the region of 2650-3100 Å, resolution $\Delta\lambda \sim 6$ Å

3. Parameters of the star and its envelope

3.1. Interstellar extinction

In the neighborhood of MWC 314 only few bright stars are found. Also we have found very few stars having MK classification and UBV photometry in the region of 1° around the object. Estimates of A_V and distances (D) towards them show that interstellar extinction starts to increase at 0.3 kpc from the Sun and reaches 4^m at 3 kpc (Fig. 8). Additionally Mel'nikov (1995) obtained UBVR photometry of 31 stars within 30″ from the object. All of them are fainter ($10\overset{m}{.}5 \leqq V \leqq 13\overset{m}{.}2$) and have much less reddening than MWC 314 (Fig. 9). The only star in this region having a comparable brightness, BD +14°3885 ($V = 9\overset{m}{.}75$), is also much less reddened ($E_{B-V} \sim 0\overset{m}{.}2$). All this implies that the object is distant and luminous. It is located at the mean reddening vector for B0-B2 super- and hypergiants (asterisks in Fig. 9) including peculiar objects like P Cyg, HD 316285, WRA 751, HD 80077. Usually their dereddened colors agree well with intrinsic ones for corresponding spectral types. Several early-B stars from the neighborhood of MWC 314 give $E_{U-B}/E_{B-V} = 0\overset{m}{.}78 \pm 0\overset{m}{.}03$. This value and the mean $B-V$ and $U-B$ of MWC 314 ($1\overset{m}{.}60$ and $0\overset{m}{.}33$ espectively, see Table 1) lead to $(B-V)_0 = -0\overset{m}{.}23$ and $(U-B)_0 = -1\overset{m}{.}09$, which corresponds to a B0 I star (Strajzhys 1977). Taking these values we get $E_{B-V} = 1\overset{m}{.}83$, $E_{U-B} = 1\overset{m}{.}43$, and $A_V = 5\overset{m}{.}7$. The intrinsic color indices are very close to those of P Cyg having T_* of 19 300 K (Lamers et al. 1983). However, we showed above that the UV SED of MWC 314 is more consistent with T_* of 25 000 and 30 000 K. This reflects the fact that optical color indices depend weakly on T_* for so hot stars. The relation between A_V and D (Fig. 8) can be used for a rough estimate of the object's radius R_*. It is more likely that the distance to-

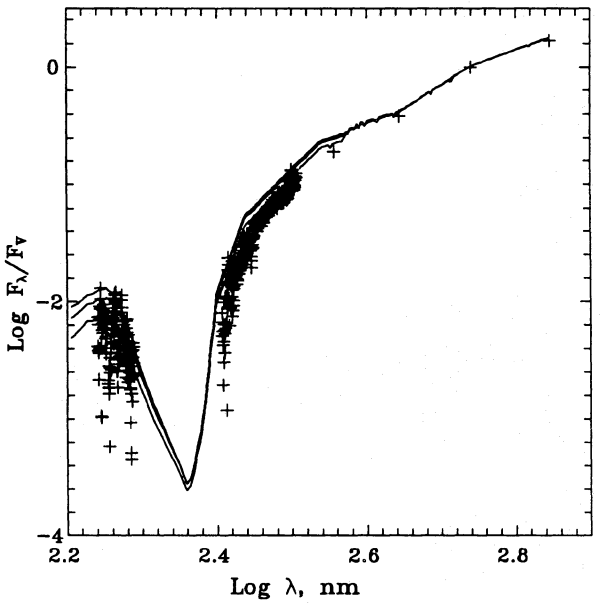

Fig. 7. Comparison of the MWC 314 SED in the UV and visual spectral region (+) with the reddened SEDs of the Kurucz models (solid lines). The model SEDs were computed with the following parameters: $T_* = 30\,000$ K, $\log g = 3.5$, $A_V = 5\overset{m}{.}7$ (upper curve), $T_* = 25\,000$ K, $\log g = 3.0$, $A_V = 5\overset{m}{.}6$ (middle curve), $T_* = 20\,000$ K, $\log g = 2.5$, $A_V = 5\overset{m}{.}5$ (lower curve).

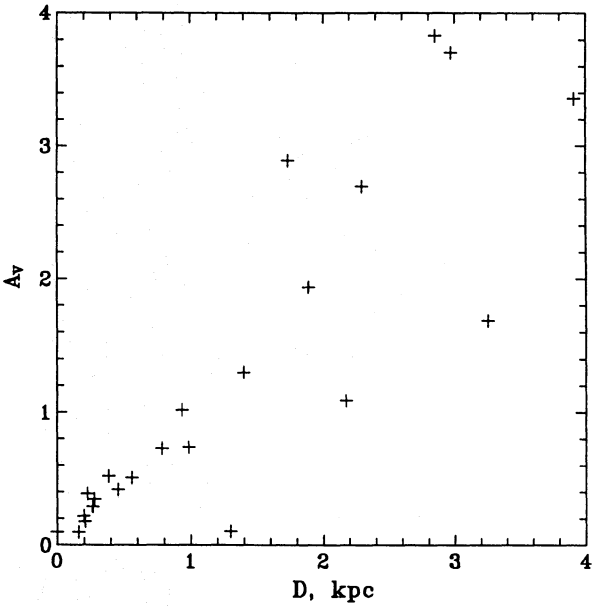

Fig. 8. The relationship between interstellar extinction and distance in the neighborhood of MWC 314

wards MWC 314 exceeds 2 kpc, because closer to the Sun the extinction is low. This value implies absolute visual magnitude $M_V < -7\overset{m}{.}2$, $R_* > 42R_\odot$ for $T_* = 25\,000$ K, and $R_* > 35R_\odot$ for $T_* = 30\,000$ K. Extrapolation of the relation leads to the distance towards the object of nearly 3 kpc which increases R_* 1.5 times. In the following sections we will try to constrain stellar parameters by modeling its envelope.

3.2. SED modeling

As seen in Fig. 1 the SED of MWC 314 is consistent with those of reddened hot stars surrounded by a gaseous envelope and with those of binary systems as well. A choice between these two possibilities depends on the value of interstellar extinction and on the contribution of the envelope to the IR continuum of the object. Since features of late-type stars have not been observed in the spectrum we try to estimate the mentioned characteristics supposing that MWC 314 is a single star. In this case, its SED at wavelengths longer than 1 μm is mainly due to free-free and free-bound radiation of the stellar wind and is affected by interstellar extinction like that of P Cyg. The ratios of fluxes at 12 and 25 μm for MWC 314 and P Cyg are practically the same (nearly 1.7) and imply no contribution of circumstellar dust. Hence, we can use the method of Lamers & Waters (1984) to fit the SED of MWC 314 . This method enables one to compute the infrared excess (IRE) radiation for isothermal stellar winds whose shape depends only on the velocity law. There are two different velocity laws usually used for high-luminosity stars. The first one was found by Van Blerkom (1978) for P Cyg from a study of Balmer lines and was used by Waters & Wesselius (1986) to fit the P Cyg IRE.

$$\begin{aligned} w(x) &= w_0 + (0.9 - w_0)\tfrac{x-1}{X_{\rm end}-1}, x \leqq X_{\rm end} \\ w(x) &= 1 - 0.1\tfrac{X_{\rm end}}{x}, x \geqq X_{\rm end} \end{aligned} \quad (1)$$

where R_* is the stellar radius, $x = r/R_*$, $w(x) = v(x)/v_\infty$, $w_0 = w(x = 1)$, $v(x)$ is the velocity at the distance x from the stellar center, v_∞ is the terminal velocity of the stellar wind. The second one is the β-velocity law of Cohen & Barlow (1977), i.e. $w(x) = w_0 + (1 - w_0)(1 - 1/x)^\beta$. It was shown to be more realistic for P Cyg by Pauldrach & Puls (1990). However, in their "current best model" wind velocity increases more slowly than than in the $\beta = 4$ velocity law and can be approximately expressed by the following formula: $w(x) \sim \log(\log x), x > 1.5$. We decided to fit the MWC 314 IRE with the β-velocity law ,the linear one, and the two following combinations of different laws:

$$\begin{aligned} w(x) &= w_0 + (1 - w_0)(1 - 1/x)^\beta, x \leqq X_{\rm end} \\ w(x) &= w(X_{\rm end}) + (1 - w(X_{\rm end}))\tfrac{x - X_{\rm end}}{X_\infty - X_{\rm end}}, x > X_{\rm end} \end{aligned} \quad (2)$$

where X_∞ is a distance at which v_∞ is reached.

$$\begin{aligned} w(x) &= w_0 + (1 - w_0)(1 - 1/x)^\beta, x \leqq X_{\rm end} \\ w(x) &= w(X_{\rm end}) + \alpha(\log(\log x)), x > X_{\rm end} \end{aligned} \quad (3)$$

where α varies between 0.2 and 0.5. The combination (2) is possibly not very realistic. However, we see no reasons to consider a more complicated one: the wavelength dependence of the MWC 314 IRE is more uncertain that for P Cyg because of its variability and of the low resolution of our optical spectra (see Sect.3.3). Since we do not know R_* and the mass loss rate

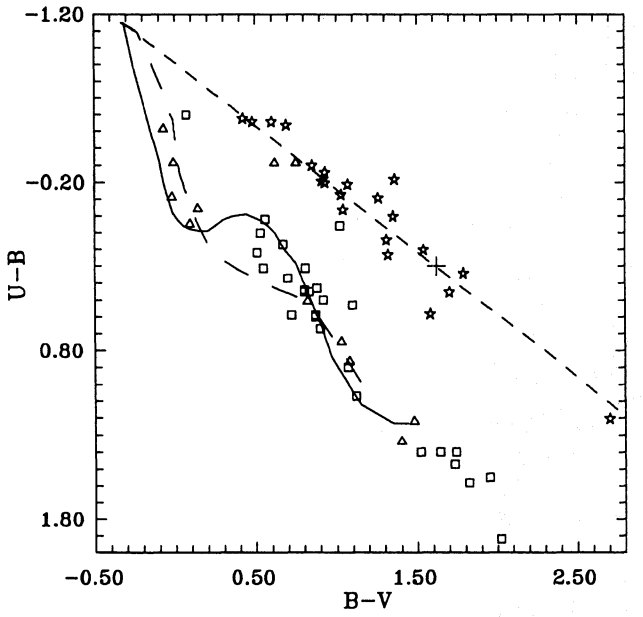

Fig. 9. Color-color diagram for stars from the neighborhood of MWC 314. △ - stars with published photometry, □ - stars measured by Mel'nikov (1995), + - MWC 314. Asterisks represent reddened early-B super- and hypergiants.

a priori, the parameters of the model are X_* from the equation (6b) of Lamers & Waters (1984), and parameters of the velocity laws.

$$X_* = 5.336\,10^{31}\,\overline{Z^2}\,\gamma\,\dot{M}^2\,T_w^{-1.5}\mu^{-2}\,v_\infty^{-2}\,R_*^{-3} \qquad (4)$$

where $\dot{M}$ is the mass loss rate in $M_\odot\,\mathrm{yr}^{-1}$, R_* is expressed in $R_\odot$, $\overline{Z^2}$ is the mean of the squared atomic charge, γ is the ratio between the number of electrons to the number of ions, μ is the mean atomic weight relative to the weight of a proton, T_w is the wind temperature in K. We used $\gamma = 1.009, \mu = 1.3, \overline{Z^2} = 1.008$. To derive the wavelength dependence of the IRE we adopted $A_V = 5\overset{m}{.}7$, the Savage & Mathis (1979) interstellar extinction law, and the Kurucz (1979) models with $T_*, \log g$ equal to 25 000 K, 3.0 and 30 000 K, 3.5 respectively. Using the wind temperature $T_w = 0.8\,T_*$ (Lamers & Waters 1984) we have computed a grid of model IREs in the range of $\lambda\lambda 0.9 - 25\mu$m. The difference between the observational and model IRE was estimated as follows:

$$\sigma = \left(\frac{\sum(1 - \frac{F_\lambda^{obs}}{F_\lambda^{mod}})}{9}\right)^{1/2} \qquad (5)$$

where F_λ^{obs} is the observational flux, F_λ^{mod} is the computed one, and the summation is over 9 wavelength bands. The linear (1) and the pure β-law gave the model IREs very different from the observational one ($\sigma > 0.1$). Better agreement was found for the laws expressed by formulae (3) ($\sigma \sim 0.05 - 0.07$) and (2) ($\sigma \sim 0.05 - 0.06$). The lowest σ were achieved with the law (2) for both stellar parameter sets with β from 0.5 to 1.2, w_0 from 0.01 to 0.05, X_{end} from 1.1 to 1.5, X_* from $2.1\,10^5$ to $2.8\,10^5$. In all models X_∞ was equal to 150 ± 3 and did not significantly affect the calculated IRE. The best results with the law (3) were obtained with the same values of β, w_0, and X_{end} as for the law (2), and α between 0.3 and 0.4. In order to put more reliable constraints on these parameter sets and to derive v_∞ and estimate $\dot{M}$ and R_* we also modelled the Balmer line profiles.

3.3. Balmer line profile modeling

We computed Balmer line profiles by means of the method described by Pogodin (1986) for spherically symmetric envelopes. In the first step of this procedure the populations of 12 lowest levels of hydrogen are computed taking into account all radiative and collisional processes (non-LTE case) in the Sobolev approximation (Pauldrach & Puls 1990 showed that it is valid for the P Cyg velocity law). In the second step we solved the radiative transfer equation by numerical integration throughout the stellar wind. Parameters of the velocity laws (2) and (3) determined in the previous subsection were used. As we noted above the main feature of the Balmer line profiles in MWC 314 is the absence of P Cyg absorption. Therefore this stellar wind must be strong enough to fill in the photospheric profiles. The terminal velocity must be neither very small to reproduce the observed line width nor very large to provide density distribution leading to high peak intensity values. On the other hand, poor spectral resolution can hide weak absorption details. Comparing Balmer line profiles of MWC 314 and P Cyg (Fig. 4) we conclude that the terminal velocity of MWC 314 should be at least by a factor of two larger than that of P Cyg, i.e. $\sim 400\,\mathrm{km\,s}^{-1}$. With these assumptions we computed a grid of models for different T_*, $\dot{M}$, R_*, and v_∞. The profiles were derived with a resolution equal to the thermal velocity (15-20 $\mathrm{km\,s}^{-1}$). For comparison with the observations we convolved them with a gaussian profile corresponding to the instrumental one to achieve a resolution of 2 Å. The best value for v_∞ was found to be about 500 $\mathrm{km\,s}^{-1}$. We estimate its uncertainty as about 10 per cent because beyond this interval differences between computed and observed profiles become significant. All models with $T_* = 25\,000$ K show peak intensities of Hα by 30 per cent smaller than the observed one while peak intensities of Hβ and Hγ were larger than observed. Models computed with $T_* = 30\,000$ K and the velocity law (3) demonstrate peak intensities of Hα and Hβ by 25-30 per cents smaller than the observed ones. Models with $T_* = 30\,000$ K and the velocity law (2) turned out to fit the observations better. The best agreement was achieved for $\beta = 0.77, w_0 = 0.02, X_{\mathrm{end}} = 1.4, R_* = 50R_\odot, \dot{M} = 3\,10^{-5} M_\odot\,\mathrm{yr}^{-1}$. The observational and model values of the line profile characteristics for the best fit are presented in Table 5. The observed and computed Hβ profiles are shown in Fig. 10. The observed Hγ is slightly fainter than the computed one which reflects simplicity of the model in comparison with reality. Hδ was obtained non-simultaneously with other Balmer lines and was not considered. R_* determined in this analysis does not contradict the value suggested in Sect.3.1. We can estimate an

Table 5. Observational and model characteristics of the MWC 314 Balmer lines

Line	Observations		Model	
	EW,Å	I_{max}/I_c	EW,Å	I_{max}/I_c
Hα	143	21.9	137	18.8
Hβ	20	4.7	20	4.5
Hγ	3.8	1.9	7	2.3

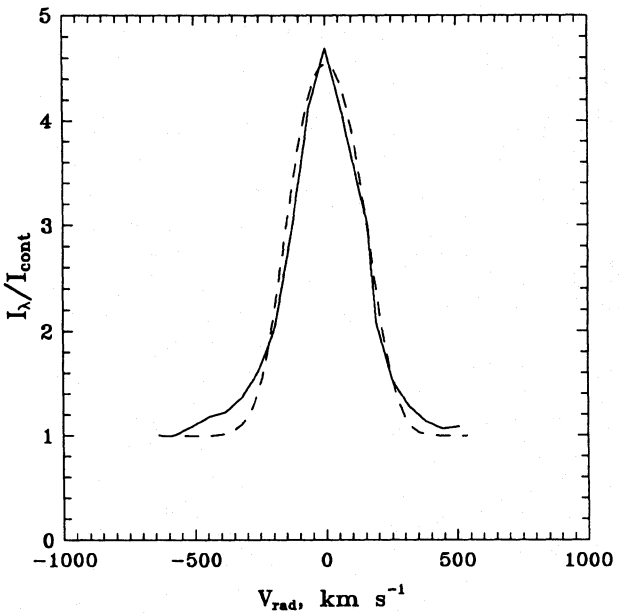

Fig. 10. Observed (solid line) and model (dashed line) Hβ profiles for MWC 314.

accuracy of its determination as nearly as 20 per cent because using $R_* = 40$ or 60 $R_\odot$ increases the difference between the model and observational profiles.

4. Discussion

The analysis carried out in the previous sections led us to estimates of intrinsic parameters of MWC 314 and its stellar wind which allowed to constrain the evolutionary status of the object. Adopting $T_* = 30\,000$ K, bolometric correction $BC = -2\overset{m}{.}9$ (Miroshnichenko & Gubotchkin 1991), and $R_* = 50 R_\odot$ we derive $M_{bol} = -10\overset{m}{.}9$ and $\log L/L_\odot = 6.2$. Further, $A_V = 5\overset{m}{.}7$ and the mean brightness $V = 9\overset{m}{.}9$ give a distance towards the star $D = 2.5$ kpc or an angular diameter $\phi = 1.7\,10^{-4}$ arcsec. The distance estimate agrees with the relation between A_V and D. The mass loss rate derived for MWC 314 is similar to those of some other early-B supergiants with strong Hα emission lines from Table 6 (e.g. HDE 316285, HD 87643, P Cyg) having $\dot{M} \geqq 10^{-5} M_\odot$ yr^{-1}. The quasiperiod of photometric variations of MWC 314 found by us is in excellent agreement with the expected one for the derived M_{bol} and T_* (Maeder 1980). We can

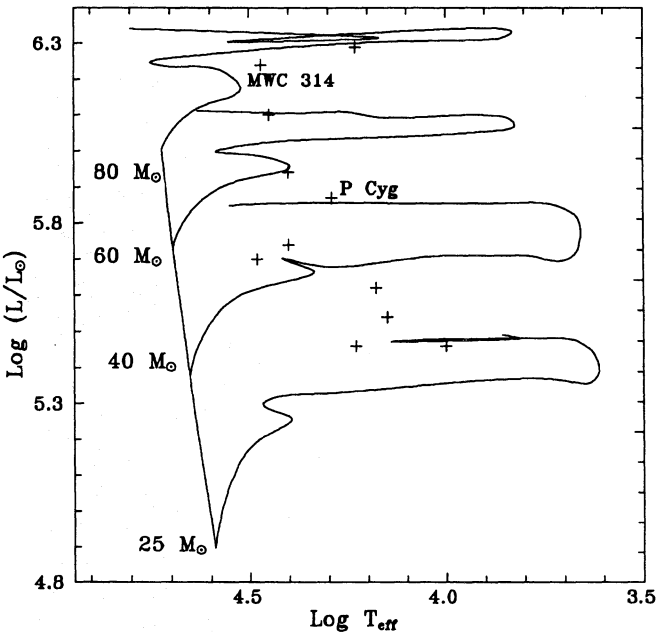

Fig. 11. HR-diagram with the positions of high-luminous stars from Table 6

also estimate a radio flux for the object using the expression given by Panagia (1987).

$$F_\nu = 1.57\,10^{11}\,\nu^{0.6}\,T_4^{0.1}\,\dot{M}^{4/3} v_\infty^{-4/3} D^{-2} \qquad (6)$$

where ν is the frequency in units of 5 GHz, T_4 is the wind temperature in units of 10 000 K, F_ν is the radio flux in mJy. The value obtained is about 6 mJy. This may be one of the ways to check our results because such a flux is easy to detect with the VLA. We cannot exclude the possibility that the object is a binary system. However, strong evidence for this has not been found so far, and we consider that the results of our study are more consistent with the case of a single star. In the present study we found that MWC 314 must be located above the ZAMS in the HR diagram and have an initial mass of nearly 80 $M_\odot$ (Fig. 11). According to Palla & Stahler (1993) such stars have no observable pre-main-sequence stage of evolution. The absence of circumstellar dust provides an additional evidence that MWC 314 is not a pre-main-sequence star because the latters are always surrounded by dust. We have shown that the structure of the object's stellar wind differs from that of normal hot supergiants. It has a low terminal velocity, and produces strong Balmer emission lines. These features are usually observed in B[e]–supergiants (Zickgraf et al. 1986) and LBVs. However, these stars have, as a rule, forbidden emission lines in their spectra. Sometimes LBVs show strong brightness variations ($\Delta V \sim 2^m$), but such episodes are alternated by periods of stability ($\Delta V \sim 0\overset{m}{.}1$). Fig. 11 shows that MWC 314 is situated close to the region of the HR diagram occupied by LBVs and B[e]–supergiants. From all this we can conclude that MWC 314 undergoes a short stage of evolution connected with a strong mass loss which can end with formation of circumstellar dust. According to Langer et al. (1994) massive

Table 6. Physical parameters of some peculiar Be stars

Object	T_*, K	R_*	M_{bol}	$\dot{M}$, $M_\odot$ yr^{-1}	Type	Reference
R 127	28,500	47	-10.5	$2.5\ 10^{-5}$	LBV	Wolf 1989
R 71	14,000	102	-9.1	$5\ 10^{-7}$	LBV	Wolf 1989
P Cyg	19,300	76	-9.9	$1.2\ 10^{-5}$	LBV	Lamers et al. 1983
HD 160529	10,000	200	-8.9	$2.5\ 10^{-5}$	LBV	Wolf 1989
MWC 314	30,000	50	-10.9	$3\ 10^{-5}$		This work
Hen S 18	25,000	39	-9.6	$3\ 10^{-5}$	B[e]	Zickgraf et al. 1989
HD 87643	17,000	63	-8.9	$1.2\ 10^{-5}$	B[e]	Lopes et al. 1992
HDE 316285	25,000	49	-10.0	$5.7\ 10^{-5}$	B[e]	Lopes et al. 1992
HR Car	15,000	98	-9.3	$8.7\ 10^{-6}$	LBV	Lopes et al. 1992
WRA 751	30,000	> 50	< -9.5	$2\ 10^{-6}$	LBV	de Winter et al. 1992
HD 80077	17,000	166	-11	$5\ 10^{-6}$		Carpay 1992

stars ($M \geqq 40 M_\odot$) can have such a stage when they pass a WN stage of evolution. The evolutionary tracks of Maeder & Meynet (1988) show that with the derived intrinsic parameters (see Table 6) MWC 314 is close to the beginning of the LBV-phase. In this case it can become the second LBV in the northern sky after P Cyg. Thus our study results in determination of physical characteristics and evolutionary status of MWC 314 . In order to improve the object's model the following observations are needed:

1. high-resolution spectroscopy for abundance estimates and improvement of spectral line profiles,
2. more frequent optical photometric monitoring to seek for possible periodicities and large-amplitude variability,
3. more sensitive mid- and far-IR photometry to check the absence of cool circumstellar dust,
4. radio flux measurements to estimate the distance.

Acknowledgements. I am grateful to Dr. A.Talavera for his help during the work with the IUE archive and hospitality during my stay at the Villafranca Satellite Tracking Station. It is a great pleasure to thank here Dr. S.Mel'nikov for obtaining photometric observations of the stars from the neighborhood of MWC 314 at the Majdanak mountain. I also thank Dr. O.Stahl for providing the digital spectrum of P Cyg. Partial support for this study was provided by the International Science Foundation (grant NS-6000).

References

Allen D.A., 1973, MNRAS, 161, 145
Balega I.I., Vereshchagina R.G., Markelov S.V., et al., 1979, Ivsestia Special. Astrofiz. Observ., 11, 248 (in Russian)
Bauer W.H., Stencel R.E., 1989, A&AS, 69, 667
Bergner Yu.K., Bondarenko S.L., Miroshnichenko A.S., Moralev Yu.D., Schumakher A.V., Yudin R.V., Yutanov N.Yu., 1988, Izvestia Glavn. Astron. Obs. v Pulkove, 205, 142 (in Russian)
Bergner Yu.K., Miroshnichenko A.S., Yudin R.V., Kuratov K.S., Mukanov D.B., Shejkina T.A., 1995, A&AS, 112, 221
Carpay J.G.H., 1992, in de Jager C. and Nieuwenhuijzen H. (eds.) "Instabilities in evolved super- and hypergiants", Proc.Intern.Colloq., 30
Cohen L., Barlow M.J. 1977, ApJ, 213, 737
Deeming T.J., 1975, Ap&SS, 36, 137
de Winter D., Pérez M.R., Hu J.Y., Thé P.S., 1992, A&A, 257, 632
Haupt H.F., Schroll A., 1974, A&AS, 15, 311
Hiltner W.A., 1956, ApJS, 2, 389
Hutsemékers D., van Drom E., 1990, A&A, 238, 134
Kurucz R.L., 1979, ApJS, 40, 1
Lamers H.J.G.L.M., de Groot M., Cassatella A., 1983, A&A, 128, 299
Lamers H.J.G.L.M., Waters L.B.F.M., 1984, A&A, 136, 37
Langer N., Hamann W.-R., Lennon M. et al., 1994, A&A, 290, 819
Lee T.A., 1970, PASP, 82, 765
Lockwood G.W., Dyck H.M., Ridgway S.T., 1975, ApJ, 195, 385
Lopes D.F., Daminieli Neto A., de Freitas Pacheco J.A., 1992, A&A, 261, 482
Maeder A., 1980, Highlights in Astronomy, 5, 473
Maeder A., Meynet G., 1988, A&AS, 76, 411
Mel'nikov S.Yu., 1995, private communication
Merrill P.W., 1927, ApJ, 65, 286
Miroshnichenko A.S., 1994, in L.A.Balona, H.F.Hendrichs, and J.M.Le Contel (eds.) Pulsation, Rotation and Mass-Loss in Early-Type Stars, Proc. Symp. IAU N162, Kluwer Acad. Publ., 396
Miroshnichenko A.S., Gubotchkin A.N. 1991, Kinematics and physics of celestial bodies, 7, 64 (in Russian)
Palla F., Stahler S.W., 1993, ApJ, 418, 414
Panagia N., 1987, Space Tel.Sci.Inst.Prepr., N 203
Pauldrach A.W.A., Puls J. 1990, A&A, 237, 409
Pogodin M.A. 1986, Afz, 24, 491
Savage B.D., Mathis J.S., 1979, Ann.Rev.A&A, 17, 73
Strajzhys V., 1977, in "Multicolor photometry of stars", Vilnius, "Mokslas"
Strajzhys V., Kurilene G., 1981, Ap&SS, 80, 353
Swennson J.W., 1942, ApJ, 97, 226
Van Blerkom D., 1978, ApJ, 221, 186
Waters L.B.F.M., Wesselius P.R., 1986, A&A, 155, 104
Winkler H., Wolf B., 1989, A&A, 219, 151
Wolf B., 1989, in Davidson K. et al. (eds.), Physics of Luminous Blue Variables, Proc. IAU Coll. 113, 91
Zickgraf F.-J., Wolf B., Stahl O., Leitherer C., Appenzeller I., 1986, A&A, 163, 119
Zickgraf F.-J., Wolf B., Stahl O., Humphreys R.M., 1989, A&A, 220, 206

This article was processed by the author using Springer-Verlag LaTeX A&A style file *L-AA* version 3.